two are corrected to 1.74 and 1.99 Å in the III phases, with only a very small change for Ge^{4+}. The cation–anion radius ratios thus become 0.305 and 0.266, respectively, and the ratio of these ratios is 1.14. This last value is consistent with the fact that the III phases discussed in this paper are of the HgI_2 and CdI_2 structure types. Eventually, if the synthesis of analogous phases of SiS_2, $SiSe_2$, $SiTe_2$, and $GeTe_2$ should be realized, the new data will permit more specific crystal–chemical analysis of the atomic parameters which determine crystal structures.

Acknowledgment. We thank Dr. H. Hasegawa of Shizuoka University for preparing the starting materials. We also thank Dr. M. Koizumi and Dr. R. Roy for their interest in this work. This work was carried out under the auspices of JSPS Grant 4R023, NSF Grant 01P74-2195B, and Materials Research Laboratory Grant DMR 74-00340.

Registry No. GeS_2, 12025-34-2; $GeSe_2$, 12065-11-1.

References and Notes

(1) C. T. Prewitt and H. S. Young, *Science*, **149**, 535 (1965).
(2) F. Dachille and R. Roy, "High Pressure Technology", R. H. Westorf, Ed., Pergamon Press, London, 1961.
(3) M. B. Myers, F. Dachille, and R. Roy. "High Pressure Measurements", A. A. Giardini and E. C. Lloyd, Ed., Butterworths, London, 1963.
(4) Ch'un-hua et al., *Dokl. Chem. (Engl. Transl.)*, **151**, 662–664 (1963) (ASTM 17-123).
(5) Ch'un-hua et al., *Russ. J. Inorg. Chem. (Engl. Transl.)*, **7**, 1117–1119 (1962) (ASTM 16-80).
(6) M. S. Silverman, *Inorg. Chem.* **5**, 2067 (1966).

Contribution from the Department of Chemistry, Northeastern University, Boston, Massachusetts 02115

Electronic and Molecular Structure of Anhydrous Ferrous Acetate. A Weak Antiferromagnet Containing Six-Coordinate Iron(II) in Nonequivalent Environments

CHRIS CHENG and WILLIAM MICHAEL REIFF*

Received February 25, 1977 AIC70142R

The temperature and field dependence of the magnetic susceptibility and iron-57 Mössbauer spectrum of anhydrous ferrous acetate have been determined over the range 1.6–300 K. These measurements show $Fe(C_2H_3O_2)_2$ to be an extended lattice antiferromagnet (2.87 K < T_{Neel} < 3.22 K) rather than a molecular dimer. Chemical isomer shift and quadrupole splitting data and near-infrared–visible optical spectra give strong evidence for a distorted FeO_6 chromophore. Zero-field high-temperature Mössbauer spectra as well as the high-field (up to 80 kG) spectra at 4.2 K clearly show the ferrous ion present in two inequivalent environments. For an applied field of 45 kG at 4.2 K the effective internal hyperfine field at these sites is ca. 230 kG. As expected x-ray powder patterns indicate that $Fe(C_2H_3O_2)_2$ is not isomorphorus with the corresponding $Cu(C_2H_3O_2)_2$ where the susceptibility of the latter compound has been redetermined to ~50 K.

Introduction

For a number of years there has been considerable interest in the chemistry of the acetates of first transition series divalent metal ions. Copper[1] and chromium[2] acetate monohydrate exist as a dimer $[M(C_2H_3O_2)_2 \cdot H_2O]_2$ which contains four bridging acetate groups. This results in a five-coordinate MO_4O' chromophore. There is ample evidence for magnetic exchange interaction between such chromophores in the dimer. However, some question arises as to whether exchange is indirect δ-symmetry superexchange via the bridging carboxylate groups or is through direct δ interaction of the metals.[3]

Our initial interest in anhydrous ferrous acetate arose from its use as a precursor for a number of other ferrous complexes. A check of the literature shows that there has been relatively little study[4] of this compound, probably owing to its instability in air. We have thus set out to characterize $Fe(C_2H_3O_2)_2$ insofar as we can, short of a single-crystal x-ray study.

Experimental Section

Anhydrous ferrous acetate can be synthesized directly by dissolving iron metal in glacial acetic acid under anaerobic conditions.[4] It can also be purchased in relatively pure form (pale buff-colored powder) from chemical supply houses packed under argon. A sample of this type was obtained from Alfa Inorganics Co. (Alfa No. 31140) and gave the following analyses: observed by the manufacturer, % C = 27.94, % H = 3.64 (calculated % C = 27.60, % H = 3.48, % Fe = 32.11); observed by Galbraith Laboratories, % C = 28.19, % H = 3.70, % Fe = 30.91 (ash). Anhydrous cupric acetate was prepared by dehydration of $Cu(C_2H_3O_2)_2 \cdot H_2O$ in a high-vacuum thermolysis apparatus at ~120 °C (<1 μ). For all of the experiments to be discussed, neat polycrystalline samples of $Fe(C_2H_3O_2)_2$ were kept in an evacuated atmosphere or under nitrogen or helium. Near-infrared visible optical spectra were obtained on a Cary 14 spectrometer for KBr pellets and fluorocarbon grease mulls in which decomposition was minimal. X-ray powder measurements were also made for samples under protective grease coating using a General Electric Co. XRD-6 powder diffractometer.

Variable-temperature magnetic susceptibility measurements were made at Northeastern University on a Faraday balance composed of a Cahn RG electrobalance, a Varian Model 4000 electromagnet with 4-in. constant-force pole caps and a Janis Super Vari-Temp cryostat over the range 1.5–300 K for ten fields between 1.6 and 5.1 kG. Temperature measurement and control were typically of the order ±0.01 K or better and were achieved using a Leeds-Northrup K-5 potentiometer and a Lake Shore Cryotronics Model DT-500 C set point controller, respectively, in conjunction with a calibrated silicon temperature sensor diode, a 10-μA constant-current source and an uncalibrated gallium arsenide control diode. Final temperature equilibration and stability were continuously monitored on a Leeds-Northrup Speedomax-XL 600-mV recorder that was used to read the error signal of the calibrated silicon diode after cancelation by the K-5 potentiometer. Temperatures below 4.2 K were measured via a vapor pressure of helium using Wallace-Tiernan Models FA-160 and 61-050 absolute-pressure gauges while pumping was precisely controlled with an L. J. Engineering Model 329 vacuum regulator valve. Temperatures below 78 K and to as low as 50 K were also achieved using liquid nitrogen by pumping (Welch 1397) to well below the triple point on solid nitrogen. Both the vapor pressure of nitrogen and a calibrated silicon diode were used to monitor the temperature. An F. W. Bell Model 610 gaussmeter with a transverse Hall probe was used for measurement of magnetic fields. The balance was calibrated with $HgCo(NCS)_4$.[5,6]

High-field Mössbauer spectra at 4.2 K were determined at the Francis Bitter National Magnet Laboratory using a niobium–tin superconducting solenoid with the magnetic field parallel to the direction of γ-ray propagation.

Mössbauer spectra in the vicinity of 4.2 K were obtained on a conventional constant-acceleration spectrometer operated in the time mode using a γ-ray source of 100-mCi ^{57}Co in a rhodium metal matrix. Temperature control was achieved using an uncalibrated silicon diode coupled to a Lake Shore Cryotronics Model DT-500 C set point controller. Temperature measurements were made with a Leeds-Northrup K-4 potentiometer or a 6-place Dana Model 5330 digital

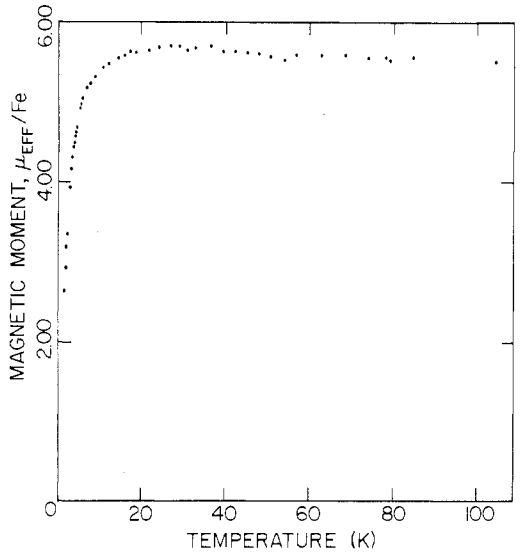

Figure 1. Temperature dependence of μ_{eff} for $Fe(C_2H_3O_2)_2$ (1.6–100 K).

Table I. Sample Magnetic Moments

T, K	μ, μ_B	T, K	μ, μ_B
302.90	5.40	5.97	5.07
188.60	5.40	5.25	4.93
160.26	5.42	4.21	4.64
113.54	5.46	3.89	4.52
79.20	5.51	3.72	4.44
68.52	5.57	3.48	4.33
48.03	5.60	3.22	4.19
32.93	5.66	2.87	3.97
26.92	5.69	2.20	3.39
18.65	5.60	2.05	3.20
16.03	5.57	1.82	2.92
8.96	5.31	1.57	2.64

voltmeter using a calibrated silicon diode driven by a 10-μA constant-current source. The temperature stability was continuously monitored by following the error signal of a silicon diode (~50 mV/K) after precise compensation via the K-4 potentiometer and was typically of the order ±0.005 K. Temperatures less than 4.2 K were obtained through controlled pumping on the Janis cryostat diffuser assembly. Least-squares–Lorentzian fits to Mössbauer spectra were accomplished using the program of Stone.[7] Anhydrous ferrous acetate exhibits a relatively strong Mössbauer effect. The percent absorption varies from ~6.5%, at 78 K (Figure 11a), to ~13.5%, at 4.2 K (Figure 9).

Results and Discussion

Magnetic Susceptibility Measurements. The effective magnetic moment of $Fe(C_2H_3O_2)_2$ as a function of temperature (1.6–100 K) is shown in Figure 1 with sample data given in Table I. The moment at high temperatures compares well with a previous[4] ambient temperature measurement and is quite reasonable for high-spin iron(II). Over the range 300–ca. 80 K, μ_{eff} is nearly constant. It then undergoes a slight rise to a maximum at ca. 25 K followed by a rapid decrease below about 10 K. These results are roughly compatible with three possibilities. (1) $Fe(C_2H_3O_2)_2$ is a simple monomeric (perhaps square-planar or tetrahedral) species exhibiting the effects of zero-field splitting at low temperatures. (2) On the other hand, it is also possible that $Fe(C_2H_3O_2)_2$ is a dimer as pictured in Figure 2a and exhibits a very weak ($|J| < \sim 0.5\ cm^{-1}$) negative intramolecular exchange. (3) $Fe(C_2H_3O_2)_2$ is an extended solid as shown in Figure 2b and exhibits low-temperature three-dimensional antiferromagnetic ordering, i.e., genuine cooperative behavior extending over the entire lattice.

Preceding choice 2 can be reasonably eliminated by comparison of the temperature dependence of the molar susceptibilities of anhydrous copper and ferrous acetates,

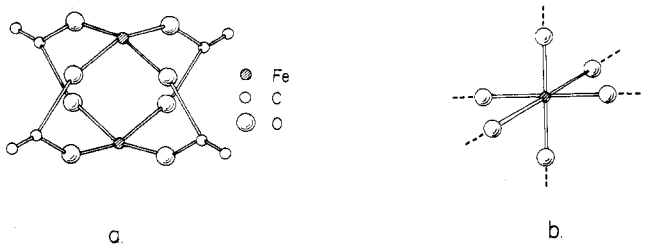

Figure 2. Possible structure of anhydrous ferrous acetate (a) as a dimer $[Fe(C_2H_3O_2)_2]_2$ and (b) as the extended lattice $[Fe(C_2H_3O_2)_2]_n$.

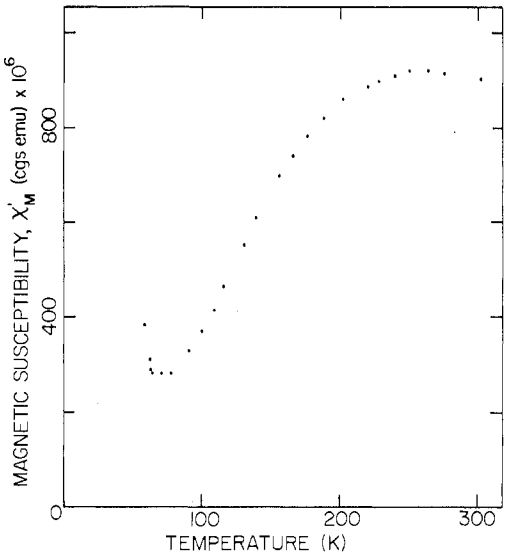

Figure 3. χ_M' vs. T for $[Cu(C_2H_3O_2)_2]_2$.

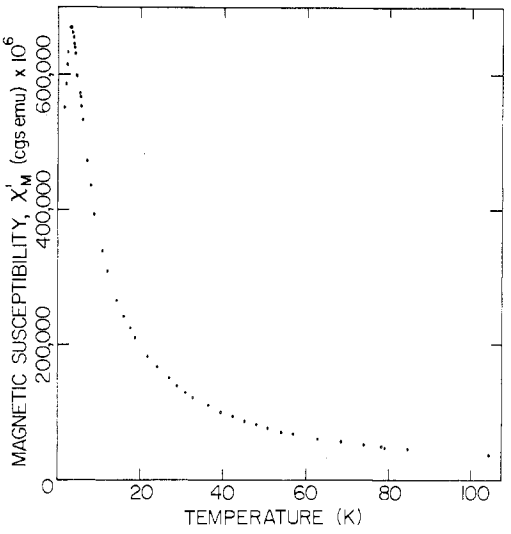

Figure 4. χ_M' vs. T for $Fe(C_2H_3O_2)_2$.

Figures 3 and 4. Anhydrous copper acetate probably has the dimeric structure of Figure 2a and may be formulated as $[Cu(C_2H_3O_2)_2]_2$. It is readily prepared by dehydration of the known[1] dimer $[Cu(C_2H_3O_2)_2 \cdot H_2O]_2$, i.e., removal of axial water to give four-coordinate CuO_4 chromophores. X-ray powder patterns of our samples of $Cu(C_2H_3O_2)_2$ and $Fe(C_2H_3O_2)_2$ suggest that they are not isomorphous. Figgis and Martin[8] have previously determined the temperature dependence of χ_M' of $Cu(C_2H_3O_2)_2 \cdot H_2O$ and $Cu(C_2H_3O_2)_2$ over the range 398–93 K. Our results for the anhydrous system generally duplicate their data over this temperature range. We have extended these data to ca. ~50 K by simply pumping on nitrogen to well below its triple point. It is seen

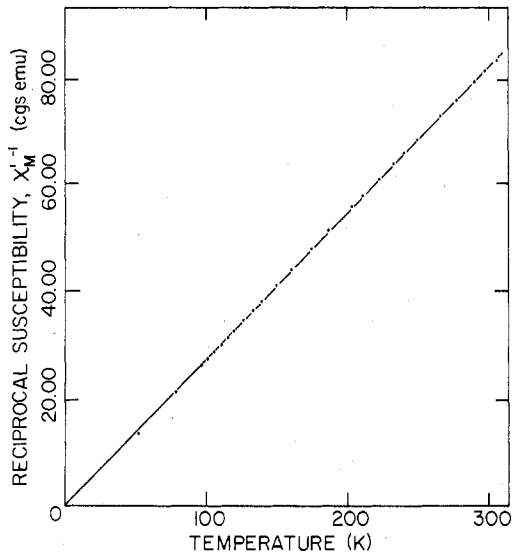

Figure 5. $\chi_M'^{-1}$ vs. T. Solid line is a least-squares fit for the Curie–Weiss parameters described in the text; T = 50–300 K; sample weight 4.65 mg.

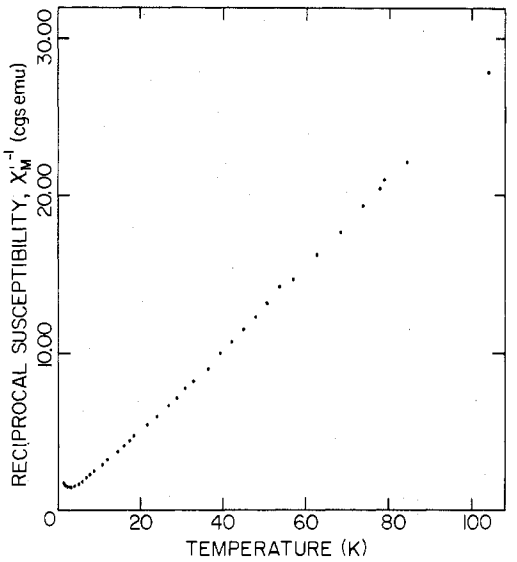

Figure 6. $\chi_M'^{-1}$ vs. T (1.6–100 K); sample weight 1.63 mg.

that at approximately 70 K χ_M' begins to increase probably owing to trace (monomeric) paramagnetic impurity. In any event, the broad, high-temperature maximum in χ_M' (~270 K) characteristic of the antiferromagnetically coupled dimer is evident. From the simple Bleaney–Bowers equation, χ_M' should level off at a constant value at ~50 K for the values of J (~−150 cm^{-1}) involved. The latter is a relatively strong exchange interaction and corresponds to a singlet–triplet separation of ~300 cm^{-1}.

For $[Cr(C_2H_3O_2)_2 \cdot H_2O]_2$ the exchange is strong enough to cause it to be diamagnetic at room temperature.[3] On the other hand, the temperature dependence of χ_M' (Figure 4) for $Fe(C_2H_3O_2)_2$ shows a sharp maximum at ~2.88 K, i.e., very weak exchange. In addition the susceptibility becomes field dependent below ca. 4 K. There is no reason to believe that if $Fe(C_2H_3O_2)_2$ does have a dimeric structure as shown in Figure 2a, it should have such weak exchange. In fact the gross magnetic properties of $Fe(C_2H_3O_2)_2$ are very reminiscent of those of ferrous formate dihydrate, $Fe(HCOO)_2 \cdot 2H_2O$, whose structure is known.[9] The latter compound has an extended lattice structure with two distinct six-coordinate ferrous sites: A sites, FeO_6 from six formate oxygens, and B sites, FeO_6 from two trans formate oxygen atoms and four in-plane water oxygens. The material exhibits a sharp antiferromagnetic maximum in χ_M' and C_M at 3.74 K and is viewed[10,11] as a two-dimensional magnetic structure owing to isolation of the A and B sites in layers.

To conclude this section, we refer to Figure 5, which shows a least-squares fit to the reciprocal susceptibility $\chi_M'^{-1}$ vs. T for $Fe(C_2H_3O_2)_2$ over the range 50–300 K for an applied field of 5.1 kG. It is evident that the material conforms to a Curie–Weiss law over this range and in fact, gives equally good least-squares fits for ten fields varying from ~1 to 5.1 kG. The results of these fits are C = 3.63 emu/mol, $\mu_{eff} = 2.828C^{1/2}$ = 5.39, and a paramagnetic Curie temperature $\Theta = -1.8 \pm 0.5$ K, consistent with the low-temperature antiferromagnetic ordering. The characteristic low-temperature minimum in $\chi_M'^{-1}$ vs. T for an antiferromagnet is seen in Figure 6. From this and the maximum of Figure 4, we estimate 2.87 K < T_{Neel} < 3.22 K. It is interesting that this system appears to obey a Curie–Weiss law since, as will be shown subsequently, there is strong evidence of two, distinct ferrous environments at both high and low temperatures. Either the sites involved are magnetically quite similar and both obey Curie–Weiss behavior or powder susceptibility measurements are not sensitive enough to detect deviations. On the other hand, both $[Cu(C_2H_3O_2)_2]_2$ and $[Cu(C_2H_3O_2)_2 \cdot H_2O]_2$ are not expected to and are not observed to obey a Curie–Weiss law. Finally, we note that there is no obvious evidence of one-dimensional magnetic interactions in terms of a broad maximum in χ_M' or significant deviation of $\chi_M'^{-1}$ from Curie–Weiss behavior at temperatures well above T_N.[12,13]

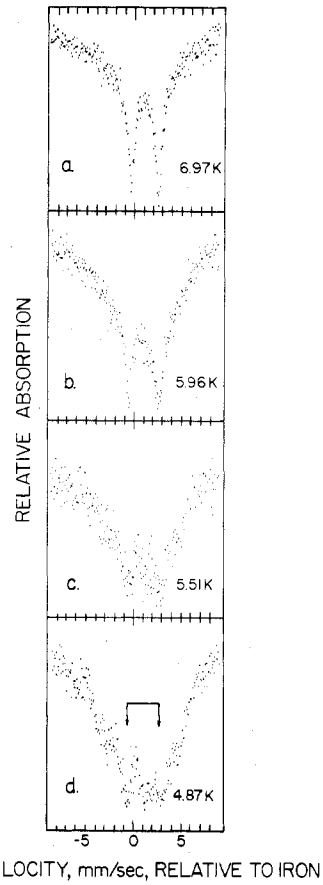

Figure 7. Temperature dependence of Mössbauer spectrum of Fe$(C_2H_3O_2)_2$: (a) 6.97 K; (b) 5.96 K; (c) 5.51 K; (d) 4.87 K.

Low-Temperature Zero-Field Mössbauer Spectra. The temperature dependence of the zero-field Mössbauer spectrum of $Fe(C_2H_3O_2)_2$ in the range 10–1.5 K is consistent with extended lattice magnetic ordering for a species such as that

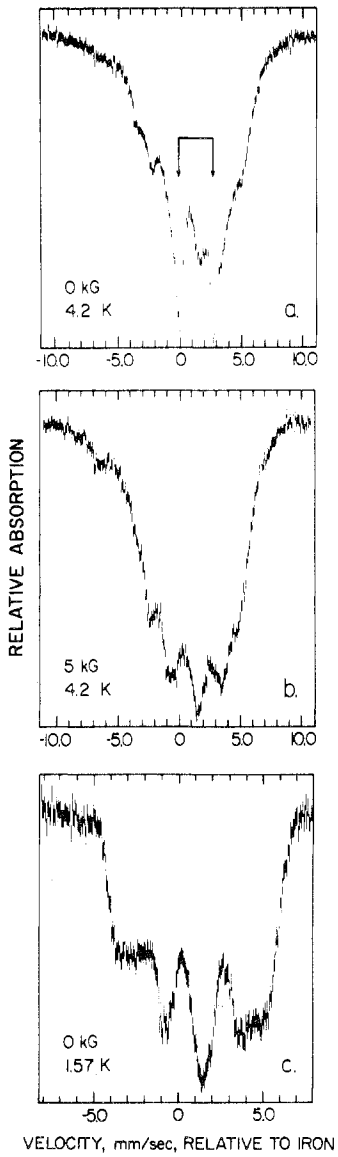

Figure 8. Mössbauer spectrum of $Fe(C_2H_3O_2)_2$: (a) 4.2 K, H_0 = 0; (b) 4.2 K, H_0 = 5 kG; (c) 1.57 K, H_0 = 0.

pictured in Figure 2b. The spectrum is seen (Figure 7) to undergo partial broadening and hyperfine splitting, *although not completely resolved*, over this temperature range. At 4.2 K, H_0 = 0, the transitions of the paramagnetic phase (arrows in Figures 8a and 7d) are seen on a broad background of unresolved hyperfine splitting. It is noteworthy that the Mössbauer spectra broadening occurs in a temperature range close to that of the sharp maximum in χ_M' suggesting magnetic ordering. The effect of decreasing the temperature to 1.5 K (H_0 = 0) is to cause the paramagnetic phase to vanish, Figure 8c. One can achieve the same effect on magnetizing with a small external field ($H_0 \approx 5$ kG) at 4.2 K, Figure 8b; but in either case fully resolved hyperfine splitting is not observed. We will return to this point in subsequent discussion of the high-field Mössbauer spectra. The spectra of Figure 8b and c are quite similar in appearance save for the fact that the spectrum at 4.2 K, H_0 = 5 kG, was measured at a higher velocity sweep and is thus somewhat compressed

The observed zero-field broadening of the Mössbauer spectrum can have its origin in either (a) slow single ion paramagnetic relaxation or (b) as mentioned, magnetic ordering. The first process could arise for a monomeric species having $D < 0$, i.e., in the case of high-spin ferrous progressive population of slowly relaxing $M_s = \pm 1$ and $M_s = \pm 2$ Kramers doublets as the temperature is decreased. However, slow paramagnetic relaxation is rare for high-spin iron(II) due to the possibility of rapid relaxation via both spin–spin and spin–lattice processes. In any event, the observed broadening with decreasing temperature is clearly not expected for anhydrous ferrous acetate formulated as an antiferromagnetically coupled dimer $[Fe(C_2H_3O_2)_2]_2$. In such a dimer, a ground state populated with decreasing temperature is a *nonmagnetic* singlet. In addition, at 1.5 K, the lowest temperature of our measurements, $kT \approx 1$ cm^{-1}. Hence, there will be little residual population and hyperfine splitting from an excited (magnetic) state of such a dimer, e.g., the triplet at $2J$ for J as small as ca. -5 cm^{-1}.

Table II. Mössbauer Parameters[a]

Compd	Temp, K		δ	ΔE	Ref
$FeCO_3$	298		1.24	1.80	15
	80		1.36	2.04	
$Fe(HCOO)_2 \cdot 2H_2O$	298	A	1.19	0.59	16
		B	1.24	2.97	
		A	1.41	1.37	
		B	1.41	3.42	
$BaFeSi_4O_{10}$	295		0.75	0.51	17
$Fe(C_2H_3O_2)_2$[b]	295	A	1.17	2.34	This work
		B	1.23	2.17	
	78		1.35	2.68	

[a] In mm/s relative to iron metal. [b] Line width (Γ) at 78 K is 0.32 mm/s.

Mössbauer Parameters and Optical Spectra. Data bearing directly on the nature of the *local iron coordination* environment of $Fe(C_2H_3O_2)_2$ are the parameters of the zero-field Mössbauer spectra and near-infrared–visible optical spectra. The chemical isomer shift is sensitive to coordination number. For iron-57, as the coordination number increases, the isomer shift increases[14] reflecting a decrease of total s-electron density at the nucleus. The isomer shift and quadrupole splitting data of $Fe(C_2H_3O_2)_2$ are given in Table II along with those[15] for $FeCO_3$, the six-coordinate A and B sites $Fe(HCOO)_2 \cdot 2H_2O$ and the four-coordinate square-planar FeO_4 site of the mineral Gillespite, $BaFeSi_4O_{10}$.[17] If anhydrous ferrous acetate were a dimer, $[Fe(C_2H_3O_2)_2]_2$ as pictured in Figure 2a, an isomer shift (δ) similar to that of Gillespite is expected. It is evident that the data for $Fe(C_2H_3O_2)_2$ suggest an FeO_6 chromophore such as pictured in Figure 2b. The type of ferrous acetate association and overall structure required to bring about such a chromophore will be evident from single-crystal x-ray study.

More convincing evidence for an FeO_6 chromophore is found in the near-infrared–visible optical spectra. These exhibit a broad d–d transition centered at ~11 000 cm^{-1} with a shoulder at ~8000 cm^{-1}. Both concentrated and dilute mulls gave no evidence for higher or lower energy d–d transitions. For an undistorted tetrahedral FeO_4 chromophore a single $^5E \rightarrow {}^5T_2$ transition is expected at ca. 5000 cm^{-1} while the square-planar FeO_4 site of Gillespite exhibits[18] d–d transitions at ca. 5000 and 12 040 cm^{-1}. In summary, the optical spectra of $Fe(C_2H_3O_2)_2$ correspond to the $^5T_2 \rightarrow {}^5E$ transition of high-spin iron(II) as an FeO_6 chromophore, split by a low-symmetry ligand field component.

High-Field Mössbauer Spectra. Mössbauer spectra in large external fields (H_0) at 4.2 K were determined to see if the material would exhibit resolved hyperfine splitting as well as approach saturation magnetization. High-spin iron(II) typically exhibits six to seven Zeeman transitions depending on the magnitude of the internal hyperfine field (H_{hf}), the degree of mixing of the M_I states involved, the magnitude of the electric field gradient tensor, and H_{hf}. With approach to saturation, the polarization of a powder sample so that the easy axes of its crystallites are along H_0 often results in diminution

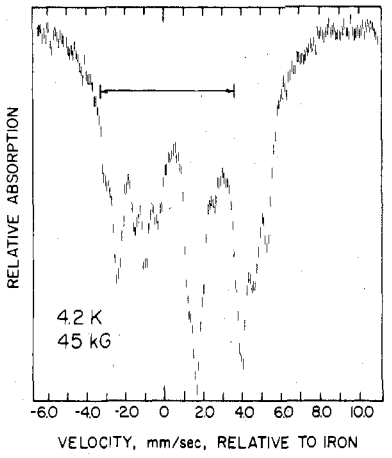

Figure 9. Mössbauer spectrum of $Fe(C_2H_3O_2)_2$ at 4.2 K, H_0 = 45 kG.

of the $\Delta M_I = 0$ transitions. The effect of a high magnetic field on $Fe(C_2H_3O_2)_2$ is seen in Figure 9. Surprisingly, instead of seeing a single six to seven transition spectrum with the expected magnetic field saturation and broadening effects, *eleven transitions* are clearly observed. The overall spectral splitting (ca. 8–9 mm/s) is about the same as those of the spectra at 1.5 K, $H_0 = 0$, and 4.2 K, H_0 = 5 kG. However, at H_0 = 45 kG the transitions are sharpened and significantly resolved. In Figure 10 the field dependence (30–80 kG) of the spectral region corresponding to ~−3 to +3 mm/s of the spectrum at 45 kG is determined at a smaller velocity sweep. The intense broad transition between +1 and +2 mm/s of Figure 9 is resolved to give three transitions for a total of thirteen. The average effective internal hyperfine field at H_0 = 45 kG is 230 kG which is reasonable for high-spin iron(II) with a quadrupole splitting of ~2.7 mm/s. The quadrupole splitting represents substantial quenching of the orbital contribution (H_L) to the internal field. Since this contribution is opposite in sign to the Fermi contact contribution, a large internal field is expected. It is reasonable to compare the internal field found here to that observed[19] for $Fe(HCO-O)_2 \cdot 2H_2O$ at its A sites (the B sites are not ordered). For the formate at 0.027 K, the effective internal field is 88 kG consistent with the smaller quadrupole splitting (1.49 mm/s) at these sites.

There are a number of possible explanations for the spectrum of Figure 9. First of all, the system is an antiferromagnet as the susceptibility data indicate. An applied field will add to the internal hyperfine field of one sublattice of an antiferromagnet and subtract from the other to give two multiple transition subspectra. Essentially this behavior is observed for *single-crystal* samples of antiferromagnets when the external field is applied along the easy axis of magnetization. However, for powder samples of an antiferromagnet in which there are all orientations of the easy axis with respect to the external field–γ-ray axis one expects and usually observes broadening rather than resolution of sublattice spectra. For critical values of the external field, a variety of isothermal, magnetically induced phase transitions can occur, e.g., spin–flop or metamagnetic transitions or canting interactions depending on the relative magnitude of the exchange and anistropy fields in the sample. However, it is again not likely that these will be observed for powder spectra.

A probable explanation for our observation of multiple hyperfine patterns at low temperatures is that $Fe(C_2H_3O_2)_2$ contains iron(II) in slightly nonequivalent environments at zero field and that this inequivalence is resolved and perhaps enhanced by a large applied field. If this is the case one might hope to observe genuine iron atom inequivalence at some

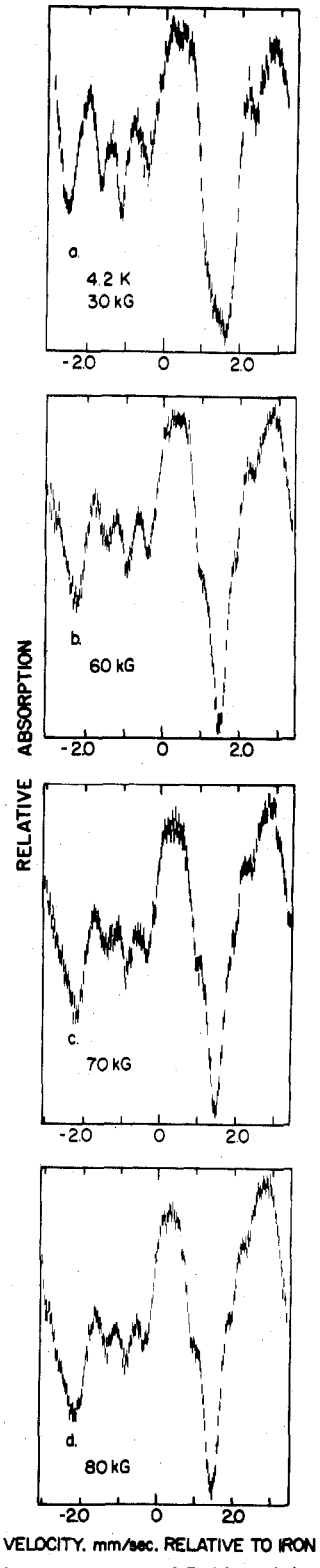

Figure 10. Mössbauer spectrum of $Fe(C_2H_3O_2)_2$ at 4.2 K (region from ca. −3 to +3 mm/s) at (a) 30 kG, (b) 60 kG, (c) 70 kG, and (d) 80 kG.

temperature for the zero-field Mössbauer spectrum of $Fe(C_2H_3O_2)_2$ where the material is a rapidly relaxing paramagnet. Precisely this observation is made at high temperatures. At 78 K (Figure 11a) what appears to be a single quadrupole doublet is observed ($\Gamma \approx 0.32$ mm/s) while at room temperature (Figure 11b) the spectrum is consistent with two overlapping doublets (A and B) each corresponding to high-spin iron(II). Trooster and De Vries[20] have made a

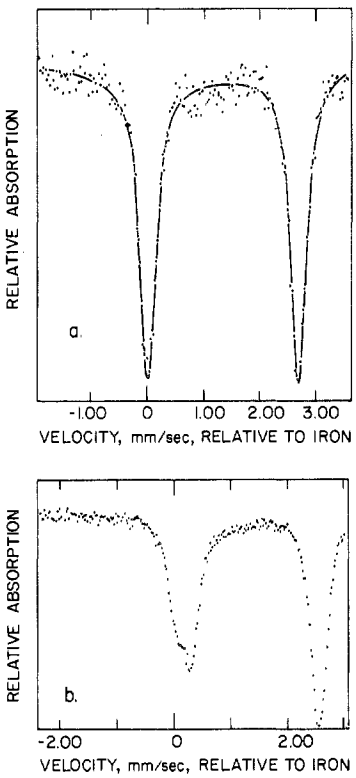

Figure 11. Mössbauer spectrum of $Fe(C_2H_3O_2)_2$: (a) 78 K; (b) ambient temperature.

similar observation and we thank them for informing us of their results. In a somewhat more detailed study of the temperature dependence above ~100 K to as high as ~370 K, they find that for $T <$ ca. 135 K essentially a single doublet is found and above this temperature the three-line spectrum as in Figure 11b is observed. It thus appears that anhydrous ferrous acetate contains ferrous ions in nonequivalent sites that can be resolved through high-temperature, zero-field Mössbauer spectra and low-temperature, high-field spectra. The exact nature of the inequivalence of the sites involved may also be ascertained through future single-crystal x-ray study.

Since completion and acceptance of the present study for publication the authors have learned of a detailed single-crystal x-ray structure determination of anhydrous cobaltous acetate.[21] This material has a complicated structure in which there are *three inequivalent Co(II) sites* designated type I, II, and III. Moreover the divalent anhydrous cobalt, *iron*, and nickel acetates are found to be isomorphous.[22] $Co(C_2H_3O_2)_2$ and $Fe(C_2H_3O_2)_2$ crystallize in the space group *Pbcn* with twenty CoO_6 chromophores per unit cell (i.e., $Z = 20$), four of type I, eight of type II, and eight of type III. There are four kinds of bridging carboxylate groups: (a) those whose oxygen atoms are each coordinated to only one cobalt atom, (b) those for which one oxygen atom is coordinated to a single cobalt atom while the other is shared by two, (c) those for which each oxygen atom is shared by two cobalt atoms, and finally (d) *chelating* carboxylate groups one of whose oxygen atoms is shared between two cobalt atoms. Type I and II cobalt sites are somewhat similar in that they each have their metal atoms coordinated to *six different* carboxylate groups from among types a, b, c, and d. While type III completes its six-coordination via ligation to four different carboxylate groups and one bidentate chelating (type d) group. From among the three types of metal sites in $Co(C_2H_3O_2)_2$, our iron-57 Mössbauer spectrum of $Fe(C_2H_3O_2)_2$ appears to distinguish two. In view of the foregoing observations for the cobalt system it seems likely that types I and II are quite similar and distinguished from type III in the Mössbauer spectrum but not from each other. Future emission Mössbauer studies of $^{57}Co(C_2H_3O_2)_2$ may be helpful in studying this aspect. In any event, the spectral areas of the inequivalent sites (approximately equal) from our and De Vries'[20] Mössbauer spectra are more consistent with types I and II rather than types II and III being essentially equivalent since that latter situation would result in the area ratio (II + III)/I ≈ 4 which is clearly inconsistent with the observed spectrum. Either of I and II or for that matter I + III essential equivalence results in the area ratio (I + II)/III ≈ 1.5, i.e., more compatible with the observed spectrum.

The overall structure of $Co(C_2H_3O_2)_2$ and thus most probably $Fe(C_2H_3O_2)_2$ consists of single CoO_6 units of type I bridging tetrameric CoO_6 groupings containing two of type II sites and two of type III.[21] This results in a complex rather open molecular structure. Thus these systems are not readily described as a simple chain, layer, or three-dimensional structure from a magnetic point of view and complex low-temperature magnetic ordering as found herein is expected.

Conclusion

The results of this work indicate that anhydrous ferrous acetate is an extended lattice type system (Figure 2b) rather than a molecular dimer as in Figure 2a. There is probably no single reason for a preference for an octahedral environment over the four-coordinate sites of a dimer. The iron will obviously be coordinatively unsaturated in the latter. An important point in comparing iron(II) to divalent copper and chromium is that the latter metals are expected to be strongly Jahn–Teller distorted in an octahedral environment while the iron should be less so. From another point of view, while Cr(II) has the ideal high-spin d^4 configuration for strong quadruple metal–metal bonding, iron may be viewed as having too many electrons. It thus possesses an inappropriate valence-shell configuration for effective metal–metal bonding, especially when the complex contains relatively nondelocalizing ligands such as acetate. The same is probably true for divalent nickel and cobalt acetates which are known[23] as M(acetate)$_2$·4H$_2$O.

Acknowledgment. W.M.R. acknowledges the support of the National Science Foundation, Division of Materials Research, Solid State Chemistry Program, Grant No. DMR 75-13592A01. He also acknowledges the partial support of the Research Corp. and HEW Grant No. RR 07143. Finally, the authors wish to express their appreciation to The Francis Bitter Magnet Laboratory, sponsored by the NSF, for use of its high-field Mössbauer spectroscopy facilities, Jan Trooster for useful discussions, and Professor D. Gonzalez Alvarez and R. Navarro for informing us of the x-ray structure determination of anhydrous cobaltous acetate.

Registry No. $Fe(C_2H_3O_2)_2$, 3094-87-9; $[Cu(C_2H_3O_2)_2]_2$, 23686-23-9.

References and Notes

(1) J. N. Van Niekerk and F. R. L. Schoening, *Acta Crystallogr.*, **6**, 227 (1953).
(2) J. N. Van Niekerk, F. R. L. Schoening, and J. F. De Wet, *Acta Crystallogr.*, **6**, 501 (1953).
(3) F. A. Cotton and G. Wilkinson, "Advances in Inorganic Chemistry", 3rd ed, Wiley-Interscience, New York, N.Y., 1972, p 919.
(4) H. D. Handt and W. Möller, *Z. Anorg. Allg. Chem.*, **313**, 57 (1961).
(5) B. N. Figgis and R. S. Nyholm, *J. Chem. Soc.*, 4190 (1958).
(6) H. St. Räde, *J. Phys. Chem.*, **77**, 424 (1973).
(7) G. M. Bancroft, A. G. Maddock, W. K. Ong, R. H. Prince, and A. J. Stone, *J. Chem. Soc. A*, 1966 (1967).
(8) B. N. Figgis and R. L. Martin, *J. Chem. Soc.*, 3837 (1956).
(9) K. Osaki, Y. Naki, and T. Watanable, *J. Phys. Soc. Jpn.*, **19**, 717 (1964).
(10) K. Takeda and K. Kowaski, *J. Phys. Soc. Jpn.*, **31**, 1026 (1974).
(11) R. D. Pierce and S. A. Friedberg, *Phys. Rev. B*, **3**, 934 (1971).
(12) L. J. De Jongh and A. R. Miedema, *Adv. Phys.*, **23**, 1 (1974).
(13) M. Steiner, J. Villain, and G. G. Windsor, *Adv. Phys.*, **25**, 87 (1976).
(14) N. N. Greenwood and T. C. Gibb, "Mössbauer Spectroscopy", Chapman and Hall, London, 1971, p 127.

(15) K. Ono and A. Ito, *J. Phys. Soc. Jpn.*, **19**, 899 (1964).
(16) G. R. Hoy and F. De S. Barros, *Phys. Rev.*, 139 (1965).
(17) M. J. Clark, G. M. Bancroft, and A. J. Stone, *J. Chem. Phys.*, **47**, 4250 (1967).
(18) R. G. Burns, M. C. Clark, and A. J. Stone, *Inorg. Chem.*, **5**, 1268 (1966).
(19) M. Shinohara, A. Ito, M. Suenaga, and K. Ono, *J. Phys. Soc. Jpn.*, **33**, 77 (1972).
(20) J. L. K. F. De Vries, Doctoral Dissertation, University of Nijmegen, 1972, p 85.
(21) R. Alcala and J. Fernandez Garcia, *Rev. Acad. Cienc. Exactas, Fis.-Quim. Nat. Zaragoza*, **28**, 303 (1973).
(22) D. Gonzalez Alvarez, M. A. Navarro, L. A. Oro, and F. Gomez Beltran, *Rev. Acad. Cienc. Exactas, Fis.-Quim. Nat. Zaragoza*, **27**, 349 (1972).
(23) J. T. Schriempf and S. A. Friedberg, *J. Chem. Phys.*, **40**, 296 (1964).

Contribution from Ames Laboratory, ERDA, Iowa State University, Ames, Iowa 50011, the Department of Chemistry, Texas A&M University, College Station, Texas 77843, and the Department of Chemistry, Auburn University, Auburn, Alabama 36803

Crystal Absorption Spectra for Potassium Octachlorodimolybdate(II) Dihydrate

PHILLIP E. FANWICK,[1a] DON S. MARTIN,*[1a] F. ALBERT COTTON,*[1b] and THOMAS R. WEBB[1c]

Received February 28, 1977 AIC70156X

Partial polarized crystal spectra are reported for $K_4Mo_2Cl_8 \cdot 2H_2O$ for both *b* and *c* polarization at 300 and 3.7 K. The intense band in the visible region, ca. 19 000 cm^{-1}, has been shown to possess molecular z-π polarization. This band was therefore assigned $^1A_{2u} \leftarrow {}^1A_{1g}$ ($\delta^* \leftarrow \delta$). It is sufficiently intense that only the absorption due to a minority fraction could be recorded. At 3.7 K, vibrational structure to the band can be resolved, but there are irregularities in the observed progression. A dipole-allowed but low-intensity transition was observed at 28 800 cm^{-1} with higher intensity in z-π polarization. It has been assigned as the $A_2' \leftarrow A_1'$ component of a $^3E_u \leftarrow {}^1A_{1g}$ transition. This is a transition to the triplet state associated with the $^1E_u \leftarrow {}^1A_{1g}$ transition seen at 31 400 cm^{-1} in pellet and mull spectra, which was shown to be polarized x, y-σ. Weak absorptions at 22 000–24 000 cm^{-1} appeared to be vibronic bands.

Introduction

The red color of the $Mo_2Cl_8^{4-}$ ion is the consequence of an electronic absorption band with a maximum at 530 nm which has been reported[2,3] for mineral oil mulls of amorphous $K_4Mo_2Cl_8$ and crystalline $K_4Mo_2Cl_8 \cdot 2H_2O$. This color is seen in freshly prepared HCl solutions of $K_4Mo_2Cl_8$, but it fades rapidly. Compounds which contain the $Re_2Cl_8^{2-}$ ion (with a $5d^8$ rather than $4d^8$ configuration) have a band at ca. 700 nm which imparts a blue color to them. Cowman and Gray[3] published the polarized crystal spectra for $[(n\text{-}C_4H_9)_4N]_2Re_2Cl_8$ in the visible region and with Mortola et al.[4] have presented extended spectra into the ultraviolet region. With the crystal structure for this compound of Cotton et al.[5] it appears clear that this transition in $Re_2Cl_8^{2-}$ is polarized in the direction of the molecular z axis, i.e., along the metal–metal bond which is aligned with the tetragonal axis of the D_{4h} molecular point group. Such polarization justifies the transition assignment as $^1A_{2u} \leftarrow {}^1A_{1g}$ ($\delta^* \leftarrow \delta$) for $Re_2Cl_8^{2-}$. Recently, Xα scattered-wave computations[2,4] for $Re_2Cl_8^{2-}$ and for $Mo_2Cl_8^{4-}$ have been performed. The ground-state ordering of the electronic orbitals for the $Mo_2Cl_8^{4-}$ ion, prepared by Norman and Kolari,[2] presented in Figure 1, implies that the lowest energy spin-allowed electronic transition should be $^1A_{2u} \leftarrow {}^1A_{1g}$ ($\delta^* \leftarrow \delta$). The calculated value for this transition in $Mo_2Cl_8^{4-}$ was 13 700 cm^{-1}, well below the observed peak at 18 900 cm^{-1}. Cowman and Gray[3] reported that the spectrum of $K_4Mo_2Cl_8$ had a richly structured band with an origin at 17 897 cm^{-1} and vibrational spacing of about 351 cm^{-1}, but they were not able to report the polarization, since they used a pellet type of multioriented sample. The present work was undertaken to determine the polarization of bands from single-crystal spectra for $K_4Mo_2Cl_8 \cdot 2H_2O$ in the visible and near-ultraviolet regions.

Experimental Section

Amorphous $K_4Mo_2Cl_8$ was prepared by the method of Brencic and Cotton.[6] Small portions of this amorphous powder were placed on a fused silica plate, and a few drops of constant-boiling (under nitrogen) HCl was added. A second plate was placed over the first plate to give a film of the HCl. The plates were then stored under H_2O-saturated nitrogen for several days until crystals of $K_4Mo_2Cl_8 \cdot 2H_2O$ had developed between the plates. Examinations of the crystals under a polarizing microscope indicated that the technique produced many diamond-shaped crystals with four-twinned quadrants and rectangular plates which gave sharp total extinctions. These rectangular plates were strongly dichroic, and the high absorption was along the long dimension of the faces.

A crystal in the form of a rectangular prism was mounted on a four-circle x-ray diffractometer and indexed using standard programs. The diffractometer indexed reflections of the crystal on the basis of orthorhombic axes $a:b:c$ = 8.019:13.302:8.053 Å, in good agreement with the structure determination of Brencic and Cotton.[7] In addition, the principal rectangular face was identified by the diffractometer as the 100 face for which the *c* axis was aligned with the long dimension of the face, i.e., with the direction of polarization for the high absorption.

The indices of refraction for the 100 face were measured by the Becke line method with a set of standard liquids supplied by the Cargille Co. The value of n_b (Na D) was 1.671 and n_c (Na D) was >1.700 (the highest index of refraction of standard set) and <1.742 (CH_2I_2).

One crystal was found with sufficiently good optical faces to provide marginal interference in the region of 664–615 nm for utilization in determination of the crystal thickness.[8] This crystal was found to be 17 ± 4 μ thick, and the thicknesses of other crystals were determined from this value and the ratio of the heights of an absorption band.

Techniques for recording spectra have been reported previously[9] with the exception that an Andonian Associates liquid-helium cryostat was employed for the low-temperature measurements. This cryostat provided He-vapor heat transfer and a germanium resistance thermometer attached to the sample mount to monitor the temperature. Temperatures below the atmospheric boiling point of He were obtained by pumping on the sample compartment.

Results and Discussion

The $Mo_2Cl_8^{4-}$ ion has the eight chlorine atoms in very nearly a cubic arrangement with the Mo–Mo bond along one of the fourfold axes of the cube, so the ion has essentially D_{4h} symmetry.[7] The $K_4Mo_2Cl_8 \cdot 2H_2O$ structure was found to be disordered in that a major fraction, 93% of the ions, have the Mo–Mo bond aligned exactly with the *c* orthorhombic axis while a minor fraction, 7%, have the Mo–Mo bond aligned at 90° to the *c* axis and 34.10° from the *b* axis.[10] the average unit cell therefore belongs to the *Pbam* space group with two $Mo_2Cl_8^{4-}$ ions per unit cell. For a transition with z or π molecular polarization, i.e., with polarization along the metal–metal bond, the crystal polarization for the majority fraction should be totally in the *c* direction for the 100 face. For the minority fraction, a π polarization will be forbidden in the *c* direction. The average square of the projection of a